LOCKHEED MARTIN ENERGY RESEARCH LIBRARIES
3 4456 0514406 4

CENTRAL RESEARCH LIBRARY
DOCUMENT COLLECTION

OAK RIDGE NATIONAL LABORATORY
CENTRAL RESEARCH LIBRARY
DOCUMENT COLLECTION
LIBRARY LOAN COPY
DO NOT TRANSFER TO ANOTHER PERSON
If you wish someone else to see this document, send in name with document and the library will arrange a loan.

OAK RIDGE NATIONAL LABORATORY
operated by
UNION CARBIDE CORPORATION • NUCLEAR DIVISION
for the
U.S. ATOMIC ENERGY COMMISSION

ORNL-TM-3366

cy. 48

DATE - August 26, 1971

Neutron Physics Division

MORSE Monte Carlo Shielding Calculations for the Zirconium Hydride Reference Reactor*

C. E. Burgart

Abstract

A comparison of DOT-SPACETRAN transport calculations and MORSE Monte Carlo calculations of a lithium-hydride and tungsten shield for a SNAP reactor has been performed. Transport of both neutrons and gamma rays was considered. Several forms of importance sampling were utilized in the MORSE calculations. Quantities internal to the shield, as well as dose at several points outside of the configuration, were in satisfactory agreement with the DOT calculations of the same.

*Presented at National Symposium on Natural and Manmade Radiation in Space, Las Vegas, Nevada, March 2-5, 1971

NOTICE This document contains information of a preliminary nature and was prepared primarily for internal use at the Oak Ridge National Laboratory. It is subject to revision or correction and therefore does not represent a final report.

This report was prepared as an account of work sponsored by the United States Government. Neither the United States nor the United States Atomic Energy Commission, nor any of their employees, nor any of their contractors, subcontractors, or their employees, makes any warranty, express or implied, or assumes any legal liability or responsibility for the accuracy, completeness or usefulness of any information, apparatus, product or process disclosed, or represents that its use would not infringe privately owned rights.

A requirement exists to provide a low radiation environment for the crew of a space station with electrical power provided by a SNAP reactor. Therefore, a shield must be designed to provide adequate protection for the crew while having the smallest possible mass.

A shadow shield consisting of lithium hydride and tungsten has been designed and optimized for a 1-MW SNAP reactor using the ASOP optimization code.[1] ASOP utilizes ANISN, a well-known one-dimensional discrete ordinates code,[2] in performing the optimization. Subsequent to the ASOP optimization of the shield, calculations have been performed using DOT, a two-dimensional discrete ordinates code,[3] and SPACETRAN, a transport code[4] for void regions, to verify that the dose constraints were met in the ASOP shield design. The optimization calculations are described in detail in reference 5. The dose constraint at the bottom of the shield 100 ft from the center of the core of the reactor was 10 mrem/hr. The dose constraint 100 ft from the center of the core at the side of the configuration was 100 rem/hr.

The MORSE Monte Carlo code[6] has been used to perform calculations for comparison with the DOT-SPACETRAN results. This code was chosen for several reasons. First, MORSE is capable of performing transport calculations in geometrically complex configurations in two and three dimensions. Second, since this problem includes transport of both primary neutrons and secondary gamma rays, MORSE's capability of performing the coupled calculation in a single job step on the computer is quite convenient. Furthermore, the ability to use the identical multigroup cross sections makes possible the checking of the transport calculations independent of the cross sections. The multigroup cross-section preparation may be investigated utilizing more energy groups or a point cross-section code

LOCKHEED MARTIN ENERGY RESEARCH LIBRARIES

3 4456 0514406 4

such as 06R.[7] However, the adequacy of the basic point cross sections may only be verified through comparison with integral and mockup experiments.

The configuration considered in these calculations is shown in Fig. 1. This is a figure of revolution about an axis along the lower edge of the figure. (Note that plus Z and 0° is to the left, minus Z and 180°, toward the crew, is to the right.) The details in the core region include: region 1, the ^{235}U and zirconium-hydride core; regions 2, 3, and 4, beryllium oxide and tantalum-tungsten reflectors and poison for the control of the reactor; region 5, the stainless-steel vessel; regions 8, the upper and lower stainless-steel grid plates; and regions 9 and 10, the upper and lower NaK coolant plenums. The shield is made up of tungsten in region 6 and lithium hydride in region 7.

The primary source of radiation for this problem was in region 1, the core of the reactor. A fission neutron source was distributed over the volume of the reactor according to previous DOT core calculations. The MORSE calculation was a fixed source calculation. Multiplication of neutrons by fission was not allowed; however, the production of fission gamma rays was allowed.

These calculations were performed in 21 neutron groups and 18 gamma-ray groups with a P_3 expansion of the angular distributions. The DOT calculations were performed with 70 discrete angles and 4500 spatial mesh points. The MORSE calculations used the identical cross sections and the identical geometry, except that in DOT the surfaces are approximated by steps in a cylindrical r-z mesh and, in MORSE, general geom is used to represent the surfaces by quadric surfaces. The energy group structure, source neutron energy spectrum, and the neutron and gamma-ray flux-to-dose conversion factors are given in Tables 1 and 2.

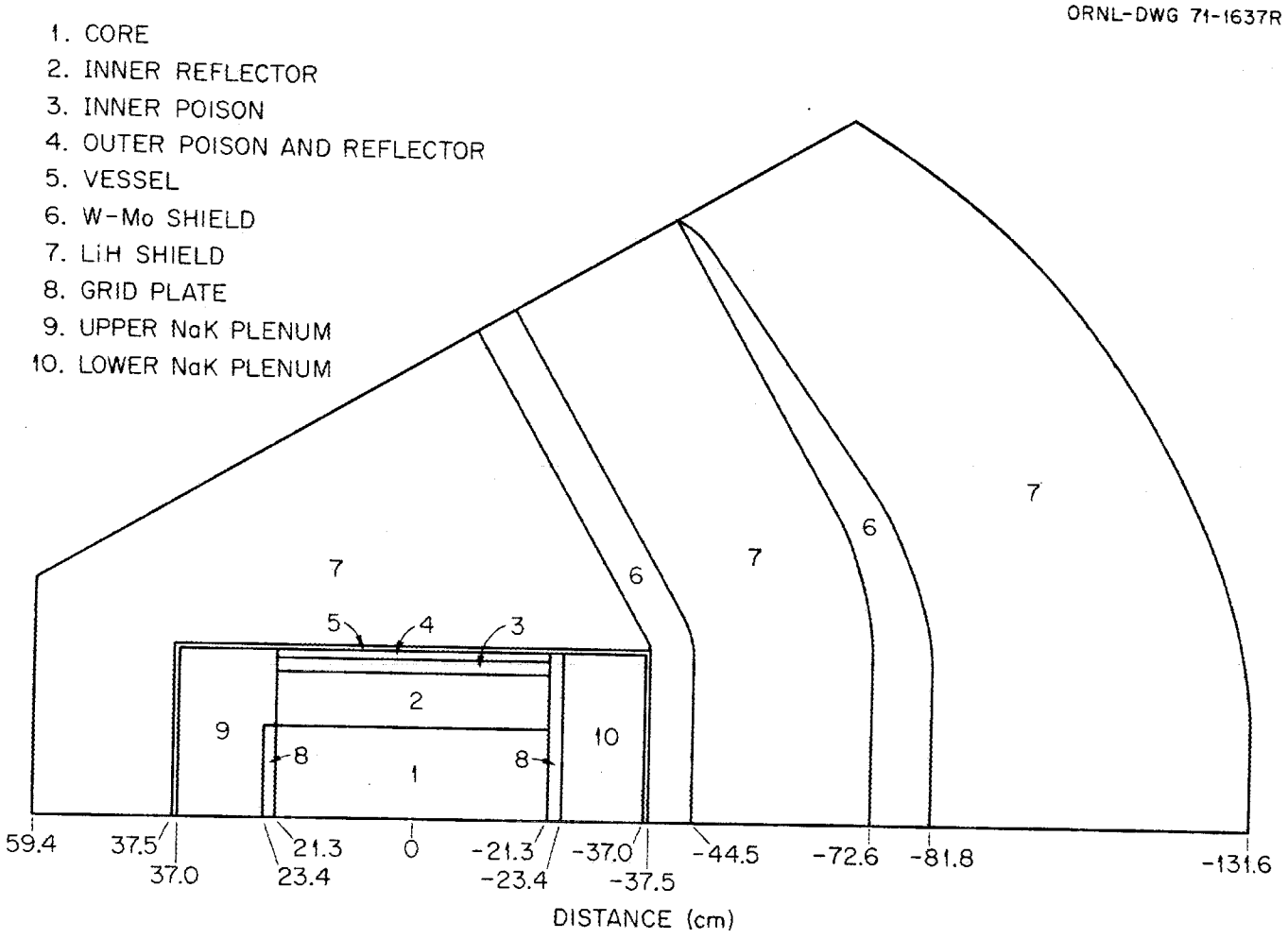

Fig. 1. Zirconium Hydride Reference Reactor Optimized 30° Shield.

Table 1. Neutron Group Structure, Source Spectrum, and Flux-to-Dose Conversion Factors

Neutron Group	Upper Energy (eV)	Source Spectrum (neutrons/sec)	Flux-to-Dose Conversion Factors [(mrem/hr)/neut/cm^2/sec]
1	14.918+6*	1.641+7	1.50-1
2	10.000+6	3.115+8	1.50-1
3	6.7032+6	2.095+9	1.37-1
4	4.4933+6	6.948+9	1.32-1
5	3.0119+6	1.428+10	1.31-1
6	2.0190+6	2.139+10	1.25-1
7	1.3534+6	2.595+10	1.16-1
8	9.0718+5	2.763+10	1.06-1
9	5.5023+5	2.763+10	1.06-1
10	3.3373+5	2.296+10	5.51-2
11	2.0242+5	1.918+10	4.01-2
12	1.2277+5	1.422+10	2.45-2
13	4.0867+4	7.654+9	8.50-3
14	1.1709+4	0.0	5.00-3
15	3.3546+3	0.0	5.00-3
16	7.4852+2	0.0	5.00-3
17	1.6702+2	0.0	5.00-3
18	3.7266+1	0.0	5.00-3
19	8.3153+0	0.0	5.00-3
20	1.8554+0	0.0	5.00-3
21	4.1399-1	0.0	3.75-3
	2.50-2		

Table 2. Gamma-Ray Group Structure and Flux-to-Dose Conversion Factors

Gamma Group	Upper Energy (MeV)	Flux-to-Dose Conversion Factors [(mrem/hr)/gr/cm^2/sec]
1	10.0	9.80-3
2	8.0	8.50-3
3	7.0	7.60-3
4	6.0	6.70-3
5	5.0	5.80-3
6	4.0	5.00-3
7	3.5	4.50-3
8	3.0	4.00-3
9	2.5	3.50-3
10	2.0	3.00-3
11	1.6	2.40-3
12	1.2	2.00-3
13	0.9	1.50-3
14	0.6	1.05-3
15	0.4	6.00-4
16	0.21	2.80-4
17	0.12	1.40-4
18	0.07	4.00-4
	0.01	

Several quantities in the core area were calculated as a check on the source description as well as the transport. One of these quantities consisted of the average neutron and gamma-ray flux in all regions inside the stainless-steel vessel. The average particle flux was calculated with MORSE utilizing a collision density estimator. Thus, the estimates far from the core or for small volumes have larger statistics. Table 3 shows the results of this comparison between DOT and MORSE. The fractional standard deviations of the MORSE results were not calculated; however, they are estimated to vary from 5 to 35%. Results are shown for both average neutron and gamma-ray fluxes. The agreement is quite good with the differences being attributed to the statistical uncertainty of the Monte Carlo calculations. The neutron results for the lower grid and lower plenum were obtained using source position biasing; therefore, the statistics of the MORSE results are quite small.

Another quantity considered was the average particle current leaving the core region through the top, side, and bottom of the stainless-steel vessel. Table 4 shows the results of this comparison. The numbers in parentheses indicate the calculated fractional standard deviations. The agreement again is quite satisfactory with all quantities lying within the statistics of the Monte Carlo calculation. The average neutron current leaving the bottom of the core region was obtained with source position biasing so that a leakage energy spectrum could be calculated with meaningful statistics in a reasonable time. This average neutron current spectrum through the bottom of the core region is shown in Fig. 2. The error bars for the MORSE results are one standard deviation. Below 370 keV, meaningful estimates were not obtained; thus, Monte Carlo results are shown for fast

Table 3. Comparison of Average Particle Fluxes in the Core Region

Region	DOT Average Flux (particles/cm^2/sec)	MORSE Average Flux (particles/cm^2/sec)
1 (Core)		
neutrons/	5.39+13*	5.50+13
gamma rays	9.43+13	9.39+13
2 (Inner Reflector)		
neutrons/	2.15+3	1.99+13
gamma rays	2.86+13	3.00+13
3 (Inner Poison)		
neutrons/	5.95+12	5.79+12
gamma rays	5.39+12	5.00+12
4 (Outer Reflector and Poison)		
neutrons/	3.47+12	3.64+12
gamma rays	2.06+12	1.94+12
8 (Upper Grid)		
neutrons/	1.36+13	2.06+13
gamma rays	1.87+13	2.36+13
8 (Lower Grid)		
neutrons/	7.83+12	7.80+12
gamma rays	9.18+12	8.31+12
10 (Lower Plenum)		
neutrons/	4.74+12	4.72+12
gamma rays	4.74+12	5.24+12
6 (First Tungsten Region)		
neutrons/	2.71+11	2.85+11
gamma rays	7.52+10	5.63+10
7 (First LiH Region)		
neutrons/	1.02+10	1.07+10
gamma rays	5.92+9	3.35+9

*Read as 5.39×10^{13}.

Table 4. Comparison of Average Particle Currents Leaving the Core Region

Surface	DOT Average Current (particles/cm^2/sec)	MORSE Average Current (particles/cm^2/sec)
Top		
neutrons/	0.96+12	1.02+12(.11)*
gamma rays	1.39+12	1.61+12(.35)
Bottom		
neutrons/	-7.01+11	-7.12+11(.03)
gamma rays	-13.6+11	-14.4+11(.21)
Side		
neutrons/	8.54+11	8.23+11(.04)
gamma rays	8.07+11	7.05+11(.18)

*Read as $1.02 \times 10^{12} \pm 11\%$.

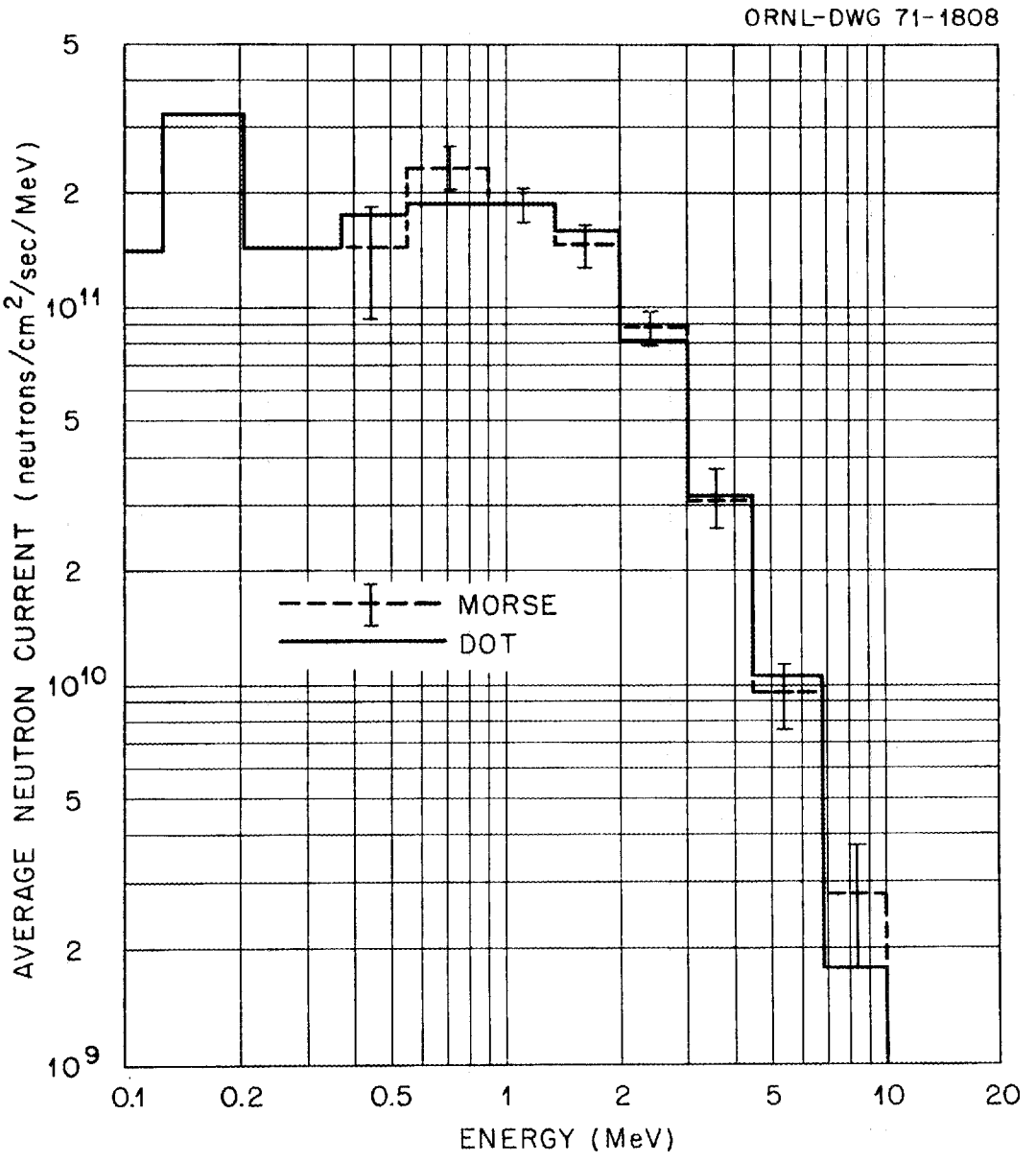

Fig. 2. Average Neutron Current Spectrum Through the Bottom of the Core Region.

neutrons only. This comparison verifies the neutron transport in this energy range through the core and sodium plenum as it affects the transport in the shield. Any subsequent discrepancy between the MORSE and DOT results must be attributed to subsequent radiation transport between this surface and the detector.

The dose at a point 100 ft from the top of the core and 100 ft from the side of the core was obtained with a minimum of importance sampling. The dose 100 ft from the center of the core at the bottom of the configuration was a very deep penetration problem and thus required much importance sampling. Without this importance sampling, the calculations of the dose at points outside the shield would have been impossible to perform. The overall attenuation of neutron dose from the center of the core to the bottom edge of the shield was approximately 3×10^{-9}. The attenuation through the shield alone was 2×10^{-8}. The attenuation of gamma-ray dose from the center of the core to the edge of the shield was approximately 6×10^{-7}. The attenuation through the shield alone was 2×10^{-6}.

The parameters used in the importance sampling were obtained from adjoint ANISN calculations. Also, the forward DOT calculations provided initial Russian roulette standards. The adjoint ANISN calculation was performed in slab geometry with the materials shown along the Z axis of the shield from the upper NaK plenum through the core and shield. The source for the adjoint ANISN calculation was the detector response at the lithium-hydride void interface. In the MORSE calculations, neutron source, energy, and position importance sampling were performed using the scalar importance calculated by ANISN in the core region. Source neutron and source secondary gamma-ray angle biasing were also performed utilizing

energy, position, and angular-dependent importance sampling. Angle biasing of the neutron and secondary gamma-ray sources was easily performed due to the assumption of isotropic emission. Reference 8 contains a more detailed explanation of the source angle biasing technique utilized. The most important importance sampling was performed in the selection of particle-flight-path lengths. A form of the exponential transform was utilized. The importance was assumed to vary exponentially along a flight path, i.e., $\exp(\mu\beta\Sigma_t\ell)$, where $\Sigma_t\ell$ is the distance through the shield in mean-free paths, and μ is the cosine of the angle between the most important direction and the direction in which the neutron is traveling. The importance sampling parameters, β, for each group and region were obtained by least-squares fitting the ANISN angular flux in the forwardmost direction with exponentials for a fixed number of mean-free paths. This was performed at each mesh point and then averaged over larger regions. For the calculation of the dose at the bottom of the shield, the direction of greatest importance was assumed to be toward $-z$ for $z > 0$ and away from a point at $z = 50$ for $z < 0$. The path-length stretching parameters can yield some insight into the particle transport in the shield. For instance, when the total neutron and gamma-ray response was used as a source for the adjoint ANISN calculation, path-length stretching parameters, $1/(1-\beta)$, for fast neutrons were on the order of from 2 to 3 for the core, first tungsten, and lithium-hydride regions, and on the order of 1.5 and less for the second tungsten region, whereas when the neutron response only was used as the source for the adjoint ANISN calculation, path-length stretching parameters on the order of from 4 to 5 were calculated for all regions until the outer edge of the shield. This indicates the relative importance

of neutrons to generating secondary gamma rays versus the importance of neutrons in contributing to the dose at the detector point.

As an aid in determining the effectiveness of the importance sampling, line-printer plots showing the location of collision sites were made during the Monte Carlo calculation.[9] Examples of neutron and gamma-ray collision site plots are shown in Figs. 3 and 4, respectively. Shown along the abcissa is the z-axis from -12 cm to 132 cm. The ordinate is the radius squared rather than the radius. Thus, the volume represented by each character is constant. The lack of a numeral indicates no collisions occurred in that cell. The numerals 1 through 0 indicate 1 through 10 or more collisions occurring in that volume. Only one out of every 20 collision sites was plotted, thus saving time and also making the plot more meaningful. These figures have a total of 70,000 collision sites shown. The amount of importance sampling was increased gradually during a sequence of Monte Carlo calculations to obtain the dose at the crew position. Thus, the possibility of overbiasing the random walk was minimized. Line-printer plots such as these were very useful in determining the effect of increased importance sampling.

Two other forms of importance sampling were also used. First, estimates were made of the dose at the bottom of the shield for only a fraction of the particle collisions occurring on the core side of the first tungsten region. When an estimate was made the weight was adjusted accordingly. Also, Russian roulette parameters were determined by observation of the number and weight of real collisions occurring in each group and in each region.

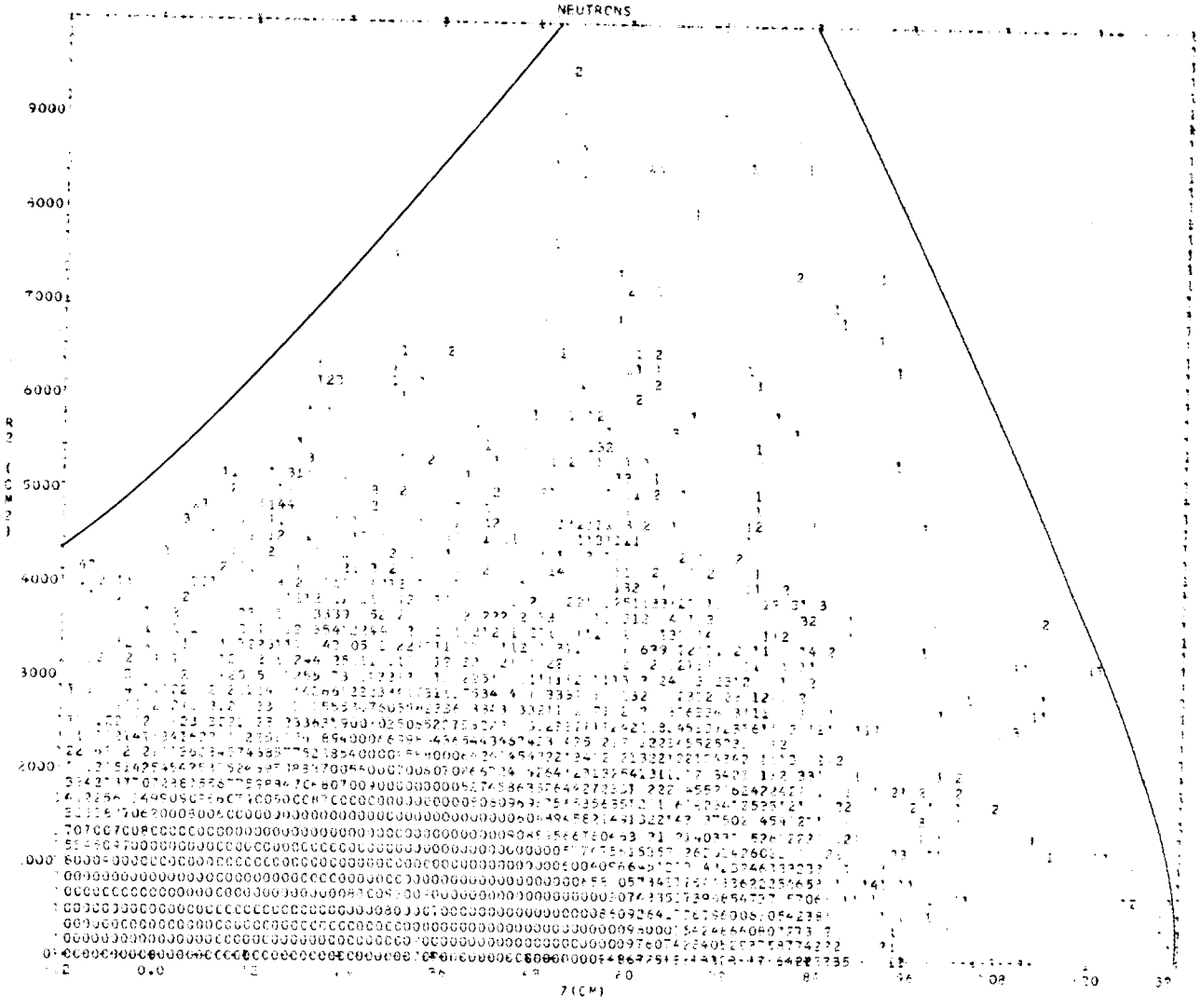

Fig. 3. Line-Printer Plot of Neutron Collision Sites for a MORSE Calculation of the Dose at the Crew Position.

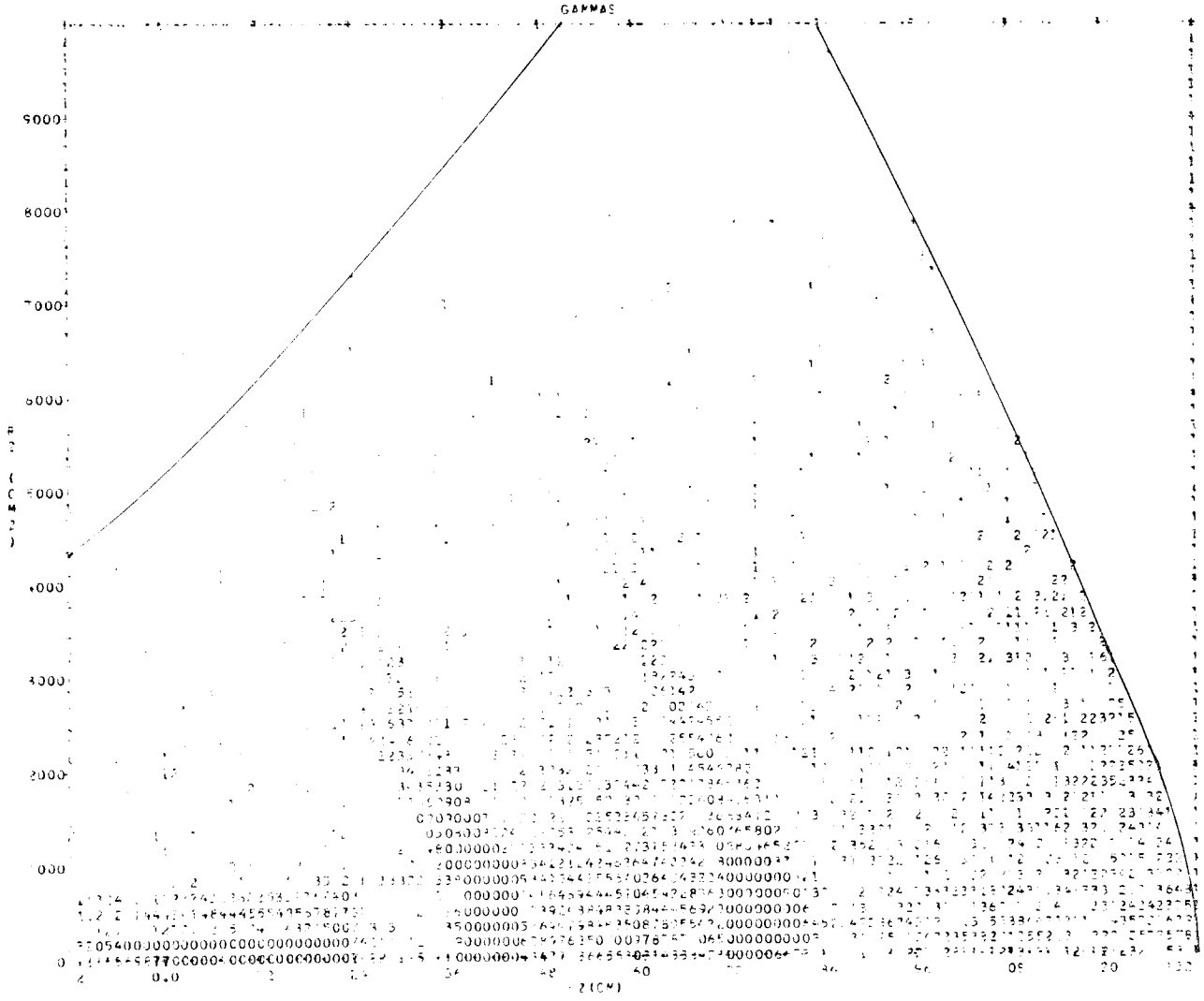

Fig. 4. Line-Printer Plot of Gamma-Ray Collision Sites for a MORSE Calculation of the Dose at the Crew Position. (This does not include secondary gamma-ray source positions.)

Estimation of the dose at the points outside the shield was performed utilizing a next-flight estimator. The results of these MORSE calculations and the DOT-SPACETRAN calculations are given in Table 5. The dose, 100 ft from the center of the core in mrem/hr, is given at several positions around the shield. The top dose, being the easiest quantity to calculate, yielded the best agreement. The DOT-SPACETRAN results fell within the statistics of the MORSE calculations. The dose falls off slightly in proceeding from 0° to 30° due to the increased thickness of the shield. At the side of the configuration, the reflectors on the reactor and the poison control drums, as well as the increased thickness of lithium hydride, contribute in making the dose somewhat less. At 90° the first tungsten region begins to have an effect, particularly on the gamma rays. The DOT-SPACETRAN results for the side of the configuration are not expected to be of highest accuracy due to the few number of discrete directions near 90°. Both neutron and gamma-ray doses calculated by DOT fall off approximately a factor of 2 between 85° and 95°. This rapid decrease may be due in part to the lack of an interpolation scheme between discrete angles in SPACETRAN. The comparison between MORSE and DOT-SPACETRAN for 90° is clouded by this falloff and the statistics on the Monte Carlo results. However, the agreement is considered to be reasonable.

The initial comparison between MORSE and DOT-SPACETRAN results (not shown in this report) for the crew position yielded approximately a factor of two discrepancy. However, on examination of the DOT calculations, two significant factors were discovered. First, the shape of the last tungsten region was considerably different than that used by MORSE. There were some relatively thin regions diagonally through the spatial mesh.

Table 5. Comparison of the Dose of Points 100 Feet From the Center of the Core

	Angle	DOT Neutron Dose	DOT Gamma Dose	DOT Total Dose	MORSE Neutron Dose	MORSE Gamma Dose	MORSE Total Dose
Top	0°				1.64+5(.10)*	1.77+5(.16)	3.41+5
	5°	1.77+5	1.75+5	3.52+5			
	10°	1.78+5	1.77+5	3.55+5			
	15°	1.75+5	1.74+5	3.49+5			
	20°	1.45+5	1.35+5	2.79+5			
	25°	1.33+5	1.47+5	2.80+5			
	30°	1.28+5	1.40+5	2.68+5			
	80°	4.54+4	7.61+4	1.22+5			
	85°	3.39+4	7.52+4	1.09+5			
Side	90°				4.60+4(.35)	3.37+4(.15)	7.97+4
	95°	1.85+4	3.51+4	5.36+4			
	100°	6.65+3	7.23+3	1.39+4			
	165°	1.25	8.42	9.67			
	170°	1.26	8.38	9.64			
	175°	1.21	8.00	9.21			
Bottom	180°				1.35(.35)	5.36(.15)	7.25

*Read as $1.64 \times 10^5 \pm 10\%$.

Second, the extrapolation across some mesh points was significantly greater than can be used with reasonable confidence. The DOT calculation was revised to more accurately represent the MORSE configuration and the spatial mesh was adjusted to reduce the number of intervals over which particle flux fell off by more than a factor of two. The revised configuration utilized in the DOT calculation is shown in Fig. 5. The DOT-SPACETRAN results shown in Table 5 are for this revised calculation. The dose at the bottom of the shield should be relatively flat from 150° to 180° due to the shadow shield nature of the configuration. The MORSE neutron dose agrees quite well with that calculated by DOT. The gamma-ray dose differs by approximately 30%. This difference is extremely small considering the total attenuation involved in the calculation; however, even this small difference could possibly be reduced by further refinements in both sets of calculations.

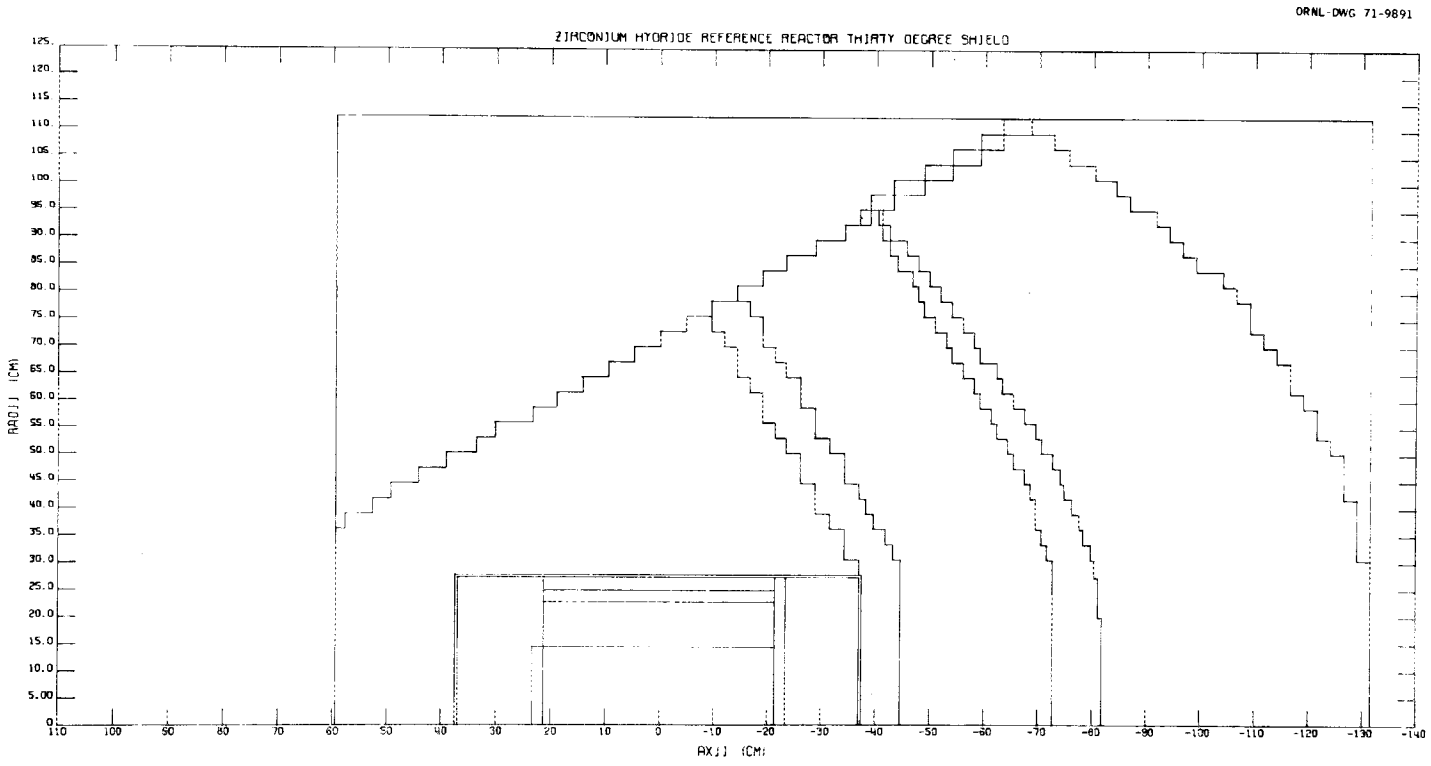

Fig. 5. Revised DOT Model of the Zirconium Hydride Reference Reactor Optimized 30° Shield.

REFERENCES

1. Ward W. Engle, Jr., "A User's Manual for ASOP, ANISN Shield Optimization Program," CTC-INF-941 (1969).

2. W. W. Engle, Jr., "A User's Manual for ANISN," K-1693 (1967).

3. W. W. Engle, Jr., "The Design of Asymmetric 4π Shields for Space Reactors," ORNL-TM-3368 (1971).

4. F. R. Mynatt, F. J. Muckenthaler, and P. N. Stevens, "Development of Two-Dimensional Discrete Ordinates Transport Theory for Radiation Shielding," CTC-INF-952 (1969).

5. S. N. Cramer and M. Solomito, "SPACETRAN - A Code to Calculate Dose at Detectors at Various Distances From the Surface of a Cylinder," ORNL-TM-2592 (1969).

6. E. A. Straker, P. N. Stevens, D. C. Irving, and V. R. Cain, "The MORSE Code - A Multigroup Neutron and Gamma-Ray Monte Carlo Transport Code," ORNL-4585 (1970).

7. C. L. Thompson and E. A. Straker, "06R-ACTIFK,Monte Carlo Neutron Transport Code," ORNL CF 69-8-36 (1969).

8. M. Solomito, Jr., "Methods of Biasing Secondary Gamma-Ray Production in Coupled Neutron Gamma-Ray Monte Carlo Calculations," presented as dissertation at The University of Tennessee.

9. E. A. Straker and M. B. Emmett, "Collision Density Plotting Routines and Collision Density Fluence Estimates for the MORSE Monte Carlo Code," ORNL-4722 (to be published).

INTERNAL DISTRIBUTION

1-3. L. S. Abbott
4. R. G. Alsmiller, Jr.
5-9. C. E. Burgart
10. A. R. Buhl
11-15. C. E. Clifford
16. S. N. Cramer
17. M. B. Emmett
18. W. W. Engle, Jr.
19. W. E. Ford, III
20. R. M. Freestone, Jr.
21. T. A. Gabriel
22. M. L. Gritzner
23. T. J. Hoffman
24. L. B. Holland
25. J. Lewin
26. R. E. Maerker
27. F. C. Maienschein
28. G. W. Morrison
29. B. J. McGregor
30. F. J. Muckenthaler
31. F. R. Mynatt
32. R. W. Peelle
33. F. G. Perey
34. J. C. Robinson
35. R. W. Roussin
36. P. N. Stevens
37. E. A. Straker
38. D. Sundberg
39. J. E. White
40. G. E. Whitesides
41. H. A. Wright
42. W. Zobel
43. E. R. Cohen (consultant)
44. H. Feshbach (consultant)
45. H. Goldstein (consultant)
46. C. R. Mehl (consultant)
47. H. T. Motz (consultant)
48-49. Central Research Library
50. ORNL Y-12 Technical Library Document Reference Section
51-53. Laboratory Records
54. Laboratory Records ORNL RC
55. ORNL Patent Office

EXTERNAL DISTRIBUTION

56. W. H. Hannum, Division of Reactor Development and Technology, U. S. Atomic Energy Commission, Washington, D. C. 20545
57. P. B. Hemmig, Division of Reactor Development and Technology, U. S. Atomic Energy Commission, Washington, D. C. 20545
58. K. O. Laughon, AEC Site Representative, ORNL
59. R. L. Detterman, Atomics International, 8900 Desota Street, Box 309, Canoga Park, Calif.
60. J. G. Gallagher, Manager, Thermal & Nuclear Design, Westinghouse Astronuclear Laboratory, P. O. Box 10864, Pittsburgh, Pa. 15236
61. G. A. Graves, N-2 Division, Los Alamos Scientific Laboratory, P. O. Box 1663, Los Alamos, New Mexico 87544
62. P. G. Johnson, Space Nuclear Propulsion Office, U. S. Atomic Energy Commission, Washington, D. C. 20545
63. I. M. Karp, Lewis Research Center, National Aeronautics & Space Administration, 21000 Brookpark Road, Cleveland, Ohio 44135
64. Capt. Dean Kaul, Defense Nuclear Agency, Washington, D. C. 20305
65. C. P. McCallum, Division of Space Nuclear Systems, U. S. Atomic Energy Commission, Washington, D. C. 20545
66. Prof. P. F. Pasqua, Department of Nuclear Engineering, University of Tennessee, Knoxville, Tenn.
67. E. A. Straker, Science Applications, Inc., Clinton Bldg., Suite 432, 2109 Clinton Ave. West, Huntsville, Ala.
68-69. Division of Technical Information Extension (DTIE)
70. Laboratory and University Division (ORO)